A membrane finite element based on position applied to the contact of fabrics with rigid surfaces

Christian L. Perlin[1], Humberto B. Coda[1]

[1]*Department of Structural Engineering, São Carlos School of Engineering, University of São Paulo*
Av. Trabalhador Sãocarlense, 400, 13566-590, São Carlos, SP, Brazil
christianperlin@usp.br, hbcoda@sc.usp.br

Abstract. In this paper, a total Lagrangian and position based formulation of membrane finite elements is employed to solve dynamic problems of contact between a non-tensioned fabric and a rigid surface. The geometric nonlinearity is naturally considered in this positional strategy, resulting in a simple description of the membrane elements by mapping gradients for the initial and current configuration. The dynamic solution is obtained by the classical Newmark-β method using alternative parameters to improve numerical stability in contact analysis. The Newton-Raphson procedure is used to solve the set of nonlinear equations. To enforce contact conditions, the penalty technique and the Lagrange multipliers are employed. A representative example for an isotropic fabric with frictionless contact is presented and results shown that the proposed numerical approach is effective for this class of problems, properly evaluating large displacements and dynamic draping.

Keywords: Membrane finite element, Fabric modeling, Positional formulation, Dynamic contact.

1 Introduction

Structural membranes are found in many applications in engineering, as building covering, parachutes, balloons and others. Membrane elements lacks flexural and compressive stiffness, being subjected predominantly to tension stresses. This system can sustain considerable loads despite its low self-weight, making it an interest alternative for several practical problems. However, the structural analysis is not as straightforward as for rigid members, and the geometric nonlinearity from large displacements must be taken into account. Moreover, techniques for the treatment of wrinkling phenomena may be necessary if non-prestressed applications are considered.

A membrane element may be subjected to contact conditions in some applications, like inflation and deflation of pneumatic structures (Li et al. [1]), deployment of foldable systems (Yuan et al. [2]) and instability situations, with the loss of stiffness leading to wrinkling (Kang and Im [3]). Contact problems are also nonlinear as the extension of the contact interface, the associated displacements and the transferred forces are unknowns. Besides, when the dynamic response is additionally required, the structural analysis become a complex task and a robust numerical formulation is essential.

In this paper, we propose a position based membrane finite element for the analysis of dynamic contact problems. The use of nodal positions as degrees of freedom, instead of displacements, allows a direct consideration of the geometric nonlinearity and a simple calculation of the deformation gradient. This alternative formulation, named Positional Finite Element Method, was presented by Coda [4] inspired by the work of Bonet et al. [5] and has been employed in the analysis of several problems. Some of them involved features of the current work, as the studies of Carvalho et al. [6], who applied the positional formulation to two-dimensional contact of elasto-plastic solids, and Siqueira and Coda [7], who analyzed dynamic problems of constrained mechanical systems. Regarding membrane applications, Coda [8] used a two-dimensional frame positional element in the analysis of inflatable structures, and Carrazedo et al. [9] considered three-dimensional membrane elements as stiffening of solid prismatic elements to model honeycomb sandwich plates. For the present work, the focus is the three-dimensional contact of membrane fabrics with rigid surfaces. The Newmark-β method is used for time integration, with suitable parameters to improve numerical stability. A node-to-surface contact discretization was employed

and the constraints were evaluated using the penalty technique and the Lagrange multipliers method. A numerical example is presented to demonstrate the effectiveness of the proposed formulation to cope with the problem.

2 Formulation

As the formulation describes the mechanical system using the nodal positions as variables, naturally considering finite displacements and rotations, nonlinear measures of strain and stresses are adopted: the Green-Lagrange strain $\boldsymbol{E}$ and the second Piola-Kirchhoff stress $\boldsymbol{S}$. The strains are calculated from initial and current mappings from a dimensionless space with a total Lagrangian description.

2.1 Membrane element kinematics

The membrane finite element is assumed in plane stress state and local coordinates are employed to define the thickness direction in space. The element is considered as a false solid, in which only the mid-surface is modeled and the displacements and stresses in the thickness direction has constant values, as it is assumed for the plane stress case. As shown in Fig. 1, the initial and current configurations (generic points P^0 and P^c, respectively) are mapped from a dimensionless space $\xi_1\xi_2\xi_3$ by:

$$\begin{aligned} \vec{f}^0\left(\xi_1,\xi_2,\xi_3\right) = x_i = X_i^\alpha \phi^\alpha\left(\xi_1,\xi_2\right) + t\xi_3 n_i^x \quad \text{and} \\ \vec{f}^1\left(\xi_1,\xi_2,\xi_3\right) = y_i = Y_i^\alpha \phi^\alpha\left(\xi_1,\xi_2\right) + t\xi_3 n_i^y, \end{aligned} \tag{1}$$

in which X_i^α and Y_i^α are the initial and current coordinates of node α in direction i, ϕ^α is the value of the shape function related to node α, considered as a Lagrange polynomial, t is the membrane thickness and n_i^x and n_i^y are the components i of the normal unitary vector in the initial and current configurations.

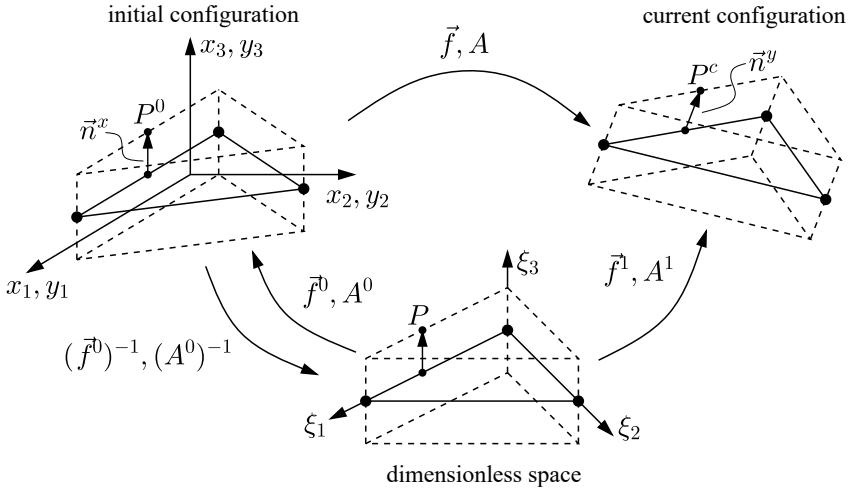

Figure 1. Configuration mappings and deformation function

Without loss of generality, considering $t = 1$ and noticing that $\xi_3 = 0$ in the mid-surface results in the following mapping gradients $\boldsymbol{A^0}$ and $\boldsymbol{A^1}$:

$$\boldsymbol{A}^0 = \begin{bmatrix} X_1^\alpha \phi_{,1}^\alpha & X_1^\alpha \phi_{,2}^\alpha & 0 \\ X_2^\alpha \phi_{,1}^\alpha & X_2^\alpha \phi_{,2}^\alpha & 0 \\ 0 & 0 & 1 \end{bmatrix} \quad \text{and} \quad \boldsymbol{A}^1 = \begin{bmatrix} Y_1^\alpha \phi_{,1}^\alpha & Y_1^\alpha \phi_{,2}^\alpha & n_1^y \\ Y_2^\alpha \phi_{,1}^\alpha & Y_2^\alpha \phi_{,2}^\alpha & n_2^y \\ Y_3^\alpha \phi_{,1}^\alpha & Y_3^\alpha \phi_{,2}^\alpha & n_3^y \end{bmatrix}. \tag{2}$$

Hence, the deformation gradient $\boldsymbol{A}$ is given by:

$$\boldsymbol{A} = \boldsymbol{A^1} \cdot \left(\boldsymbol{A^0}\right)^{-1}. \tag{3}$$

The strains $\boldsymbol{E}$ and stresses $\boldsymbol{S}$, considering the Saint-Venant-Kirchhoff constitutive model, are calculated using the expressions:

$$\boldsymbol{E} = \frac{1}{2}\left(\boldsymbol{A}^t \cdot \boldsymbol{A} - \boldsymbol{I}\right) \quad \text{and} \quad \boldsymbol{S} = \mathbb{C} : \boldsymbol{E}, \tag{4}$$

where $\boldsymbol{I}$ is the identity tensor and $\mathbb{C}$ is the constitutive tensor, which is the same used in the classical Hooke's Law.

2.2 Motion equations and time integration procedure

The Positional Finite Element Method employs the principle of stationary potential energy to describe the motion of the system. According to this principle, the system is at equilibrium (static or dynamic) when the first variation of the total potential energy Π is zero. For the problem in consideration, the total energy comprises the potential of external applied forces P, assumed here as conservatives, the strain energy U, the kinetic energy K and a potential C related to contact, or $\Pi = P + U + K + C$. The first variation of Π results in the system of motion equations:

$$\delta\Pi = \delta P + \delta U + \delta K + \delta C = \left(\frac{\partial P}{\partial \vec{Y}} + \frac{\partial U}{\partial \vec{Y}} + \frac{\partial K}{\partial \vec{Y}} + \frac{\partial C}{\partial \vec{Y}}\right)\delta\vec{Y} = 0 \quad \therefore \quad \frac{\partial P}{\partial \vec{Y}} + \frac{\partial U}{\partial \vec{Y}} + \frac{\partial K}{\partial \vec{Y}} + \frac{\partial C}{\partial \vec{Y}} = \vec{0}, \tag{5}$$

with δ denoting variation and $\vec{Y}$ being the vector of current nodal positions.

The four vectors of eq. (5) are, respectively, the external applied force, the internal force, the inertial force and a contact force. Solving this nonlinear system using the Newton-Raphson procedure, eq. (5) is rewritten as:

$$\vec{G}\left(\vec{Y}\right) = -\vec{F}^{ext} + \vec{F}^{int} + \vec{F}^{inert} + \vec{F}^{cont} = \vec{0}, \tag{6}$$

where $\vec{G}$ is an unbalanced force vector, equals to zero in an exact solution. The solution is obtained iteratively by:

$$\boldsymbol{H} \cdot \Delta\vec{Y} = -\vec{G}\left(\vec{Y}^0\right), \tag{7}$$

where $\boldsymbol{H}$ is the Hessian matrix of the system, given by the derivative of the force vector $\vec{G}$, $\vec{Y}^0$ is a first solution attempt and $\Delta\vec{Y}$ is the correction in the nodal positions. The procedure stops when this correction becomes small according a tolerance tol defined by the user, evaluated as $\|\Delta\vec{Y}\|/\|\vec{X}\| \leq tol$.

To complete the description of the problem, the first and second derivatives of the energy potentials must be calculated. The contact potential C depends on the method used for constraint enforcement and will be presented in section 2.3. Noticing that the first derivative of P (vector $-\vec{F}^{ext}$) is an input data, it is possible to rewrite eq. (6) as:

$$-\vec{F}^{ext} + \int_{V_0} \boldsymbol{S} : \frac{\partial \boldsymbol{E}}{\partial \vec{Y}}\, dV_0 + \boldsymbol{M}\ddot{\vec{Y}} + \vec{F}^{cont} = \vec{0}, \tag{8}$$

where $\boldsymbol{M}$ is the mass matrix and the dot indicates time derivative.

One must express accelerations and velocities in terms of positions to solve the system of equations. Adopting the well known Newmark-β method for time integration, positions and velocities at the current time step $s+1$ are given by:

$$\vec{Y}_{s+1} = \vec{Y}_s + \Delta t \vec{\dot{Y}}_s + \left(\frac{1}{2} - \beta\right) \Delta t^2 \vec{\ddot{Y}}_s + \beta \Delta t^2 \vec{\ddot{Y}}_{s+1}, \tag{9}$$

$$\vec{\dot{Y}}_{s+1} = \vec{\dot{Y}}_s + (1 - \gamma)\, \Delta t \vec{\ddot{Y}}_s + \gamma \Delta t \vec{\ddot{Y}}_{s+1}, \tag{10}$$

in which β and γ are parameters of the method and Δt is the time step.

The most common set of values is $\beta = 0.25$ and $\gamma = 0.5$, corresponding to constant acceleration throughout the time step (trapezoidal rule). However, these parameters may imply in difficulties in convergence for dynamic contact problems due to high-frequency oscillations, induced by sudden changes of forces and accelerations. It is desirable to damp out these spurious high-frequency modes, what can be achieved modifying β and γ to introduce a numerical damping to dissipate the energy associated with these modes. We used here the values of $\beta = 1.0$ and $\gamma = 1.5$ suggested by Hu [10]. This numerical dissipation depends on the time step adopted, so smaller time steps must be used in order to maintain the accuracy of the analysis.

Using eq. (9) and eq. (10) in the derivatives of eq. (8), the Hessian matrix of the system can be calculated with:

$$\boldsymbol{H} = \int_{V_0} \frac{\partial \boldsymbol{S}}{\partial \vec{Y}} : \frac{\partial \boldsymbol{E}}{\partial \vec{Y}} + \boldsymbol{S} : \frac{\partial^2 \boldsymbol{E}}{\partial \vec{Y} \otimes \partial \vec{Y}}\ dV_0 + \frac{\boldsymbol{M}}{\beta \Delta t^2} + \boldsymbol{H^{cont}}, \tag{11}$$

where $\boldsymbol{H^{cont}}$ is the contribution in the Hessian due to the contact potential.

2.3 Contact enforcement

The contact model adopted allows only compression forces between the interfaces, i. e., there is no adhesion or friction. A node-to-surface discretization was employed, considering nodes as projectiles and element surfaces as targets. The contact detection was evaluated using the oriented distance g (gap function) calculated by:

$$g = \left(\vec{y}^P - \vec{y}^{P'}\right) \cdot \vec{n}, \tag{12}$$

in which $\vec{y}^P$ are the coordinates of the projectile, $\vec{y}^{P'}$ are the coordinates of the projectile's projection over the target surface and $\vec{n}$ is the normal unitary vector.

Once a pair node-surface has become into contact, the respective contribution to the force $\vec{F}^{cont}$ and to the Hessian $\boldsymbol{H^{cont}}$ must be added. The contact constraints were evaluated using two different methods: the penalty technique and the Lagrange multipliers. The penalty technique satisfies the impenetrability condition only approximately, depending on a parameter η which must be calibrated. In this method, the potential C is written as:

$$C = \frac{1}{2} \eta g^2. \tag{13}$$

The method of Lagrange multipliers enforces the impenetrability condition exactly using multipliers λ to add the constraints to the system of equations, increasing its size. These multipliers represents the contact force in the interface, so the potential C is given by:

$$C = \lambda g. \tag{14}$$

2.4 Wrinkling model

Due to the very low compressive stiffness of membrane, wrinkles and folds occurs before compressive stresses could arise. In cases when a membrane element may be subjected to this conditions (a fabric without an initial prestress, for instance), a wrinkling model must be used to avoid compression and evaluate the stresses in a more consistent way. In this work, we used a simple model based on the tension field theory and adopting a stress criterion to evaluate the status of the membrane (taut, wrinkled or slack). The calculations are made as follows: (1) the principal stresses and directions of the tensor $\boldsymbol{S}$ are calculated, i. e., the tensor is rotated to the principal directions; (2) negative principal stresses are set to zero, therefore only tension stresses are considered; (3) the tensor is rotated back to the original directions using the principal directions previously calculated. A similar model was used by Pauletti and Rocha [11], which obtains the same results using an operationally different approach.

3 Numerical example: square fabric falling over a base

We present here a numerical example to illustrate the proposed formulation. The example consists in a square fabric, with sides of 20 cm, falling over a rigid square pedestal with sides of 10 cm, with an initial height of 5 cm between the planes. A uniform load of 1.8816 N/m^2, representing self-weight, induces motion and subsequent draping of the membrane over the pedestal. For the fabric, it was considered elastic modulus $\mathbb{E} = 2$ MPa, Poisson coefficient $\nu = 0.3$, specific weight $\rho = 320$ kg/m^3 and thickness $t = 0.6$ mm. Figure 2 depicts the employed discretization in 800 triangular membrane elements with linear interpolation.

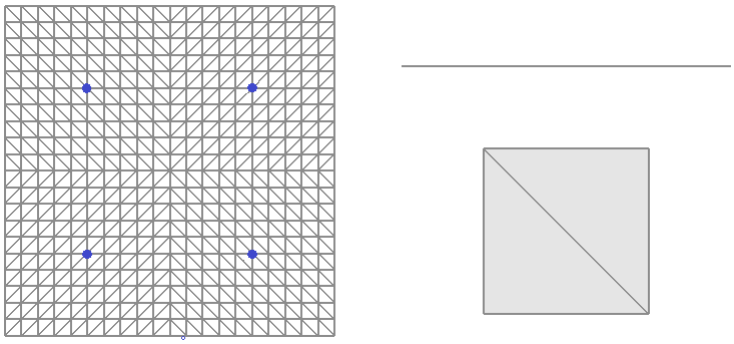

Figure 2. Discretization of the numerical example in top and lateral views. Blue dots indicates the base corners.

The time integration procedure was discretized in 10 steps of 0.01 s plus 450 steps of 0.0001 s, using the Newmark-β method with $\beta = 1.0$ and $\gamma = 1.5$, as suggested by Hu [10]. Contact occurs at time $t = 0.1011$ s. No viscous damping was considered; the damping is provided only by the dynamic algorithm. Both penalty and Lagrange multipliers methods were used, the first considering $\eta = 5 \cdot 10^4$ N/m.

Vertical displacements for selected time steps are depicted in Fig. 3, using the penalty technique to enforce contact conditions. For the Lagrange multipliers method, values are similar. It can be seen that the positional formulation evaluates correctly the draping of the membrane over the base, even with large displacements, and the wrinkling model adopted eliminates compression and ensures a proper calculation of stresses. Due to numerical damping, membrane's lifting after contact with the base is negligible. When reaching the final steps of the analysis, the corners of the fabric begin to fold and self-contact is observed.

An attentive look at the final displaced configuration shown in Fig. 3 reveals that the calculated response is not perfectly symmetric - some of corner's folds are slightly larger than others. The reason is that this problem is very sensitive in a numerical sense. As the fabric does not have an initial prestress, the static Hessian (the integral term in eq. (11)) is singular. The dynamic analysis is possible due to the mass matrix (not singular) added to the Hessian; however, usually membrane elements have a very low self-weight and the contact contribution $\boldsymbol{H}^{cont}$ for large contact forces may produce a destabilizing effect in the system of equations, and a little (in the example, almost imperceptible) difference for symmetric points response can occur.

A comparison of values obtained from the two contact enforcement methods reveals straight proximity between results, but a small difference could be noted in the displacements of the fabric's node above the base's corner after t =0.125 s. While the node remains over the base when using Lagrange multipliers, in the analysis with the penalty technique the node begins a slightly penetration to the base, reaching position $y_3 = -0.05347$ m

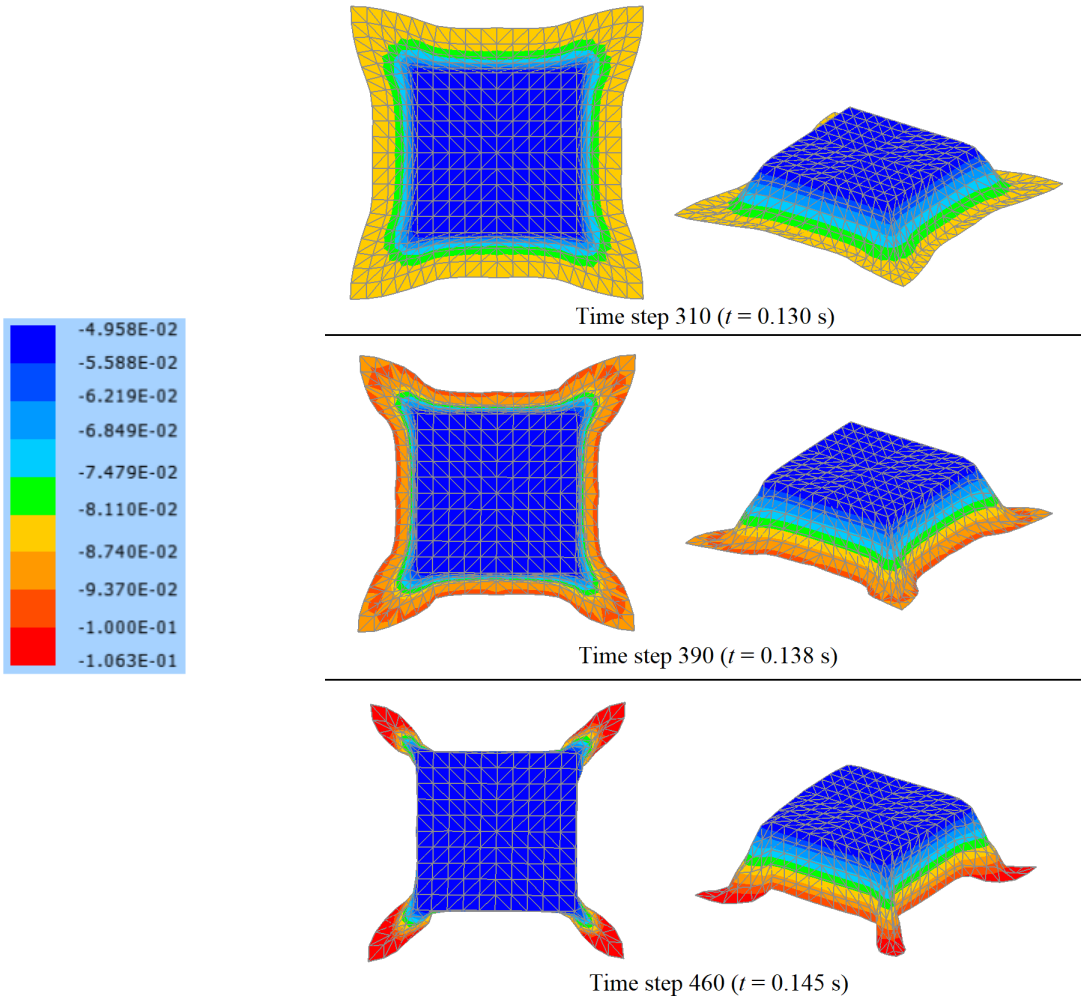

Figure 3. Vertical displacements (in m) in top and perspective views for selected time steps

at the final time step. This difference may be explained by the numerical sensitivity of the system, which is greater in the penalty method due to the large values of η used to enforce contact.

4 Conclusions

In this paper, we employed an alternative formulation of the Finite Element Method in the analysis of membranes under dynamic contact. This formulation uses positions as main variables, intrinsically accounting for the geometric nonlinearity. The membrane positional element is considered as a false solid, resulting in a simple calculation of the deformation gradient. Results from a numerical example of an isotropic fabric illustrates the ability of the formulation in deal with large displacements and contact nonlinearities, even in the dynamic case. Further steps in the research will include other types of finite elements, such as solids and shells, and more refined time integration methods.

Authorship statement. The authors hereby confirm that they are the sole liable persons responsible for the authorship of this work, and that all material that has been herein included as part of the present paper is either the property (and authorship) of the authors, or has the permission of the owners to be included here.

References

[1] Q. Li, X. Guo, Q. Qing, and J. Gong. Dynamic deflation assessment of an air inflated membrane structure. *Thin-Walled Structures*, vol. 94, pp. 446–456, 2015.

[2] T. Yuan, Z. Liu, Y. Zhou, and J. Liu. Dynamic modeling for foldable origami space membrane structure with contact-impact during deployment. *Multibody System Dynamics*, vol. 50, n. 1, pp. 1–24, 2020.
[3] S. Kang and S. Im. Finite element analysis of dynamic response of wrinkling membranes. *Computer Methods in Applied Mechanics and Engineering*, vol. 173, n. 1, pp. 227–240, 1999.
[4] H. B. Coda. An exact FEM geometric non-linear analysis of frames based on position description. In *17th International Congress of Mechanical Engineering (COBEM 2003)*, 2003.
[5] J. Bonet, R. Wood, J. Mahaney, and P. Heywood. Finite element analysis of air supported membrane structures. *Computer Methods in Applied Mechanics and Engineering*, vol. 190, n. 5, pp. 579–595, 2000.
[6] P. R. P. Carvalho, H. B. Coda, and R. A. K. Sanches. Positional finite element formulation for two-dimensional analysis of elasto-plastic solids with contact applied to cold forming processes simulation. *Journal of the Brazilian Society of Mechanical Sciences and Engineering*, vol. 42, n. 5, 2020.
[7] T. M. Siqueira and H. B. Coda. Total Lagrangian FEM formulation for nonlinear dynamics of sliding connections in viscoelastic plane structures and mechanisms. *Finite Elements in Analysis and Design*, vol. 129, pp. 63–77, 2017.
[8] H. B. Coda. Two dimensional analysis of inflatable structures by the positional FEM. *Latin American Journal of Solids and Structures*, vol. 6, n. 3, pp. 187–212, 2009.
[9] R. Carrazedo, R. R. Paccola, and H. B. Coda. Active face prismatic positional finite element for linear and geometrically nonlinear analysis of honeycomb sandwich plates and shells. *Composite Structures*, vol. 200, pp. 849–863, 2018.
[10] N. Hu. A solution method for dynamic contact problems. *Computers & Structures*, vol. 63, n. 6, pp. 1053–1063, 1997.
[11] R. M. O. Pauletti and K. B. Rocha. A simple finite element framework for modelling pneumatic structures. *Engineering Structures*, vol. 235, pp. 111812, 2021.